A SMALL APERTURE SEISMO-ACOUSTIC ARRAY
Signal Assessment

Brian Stump,Chris Hayward, and Sara Mihan House, Southern Methodist University
Myung-Soon Jun and Jeong-Soo Jeon, Korea Institute of Geology, Mining and Materials

Sponsored by Defense Threat Reduction Agency
Contract No. DSWA01-98-C-0131

ABSTRACT

The Korea Institute of Geology, Mining, and Materials and Southern Methodist University jointly designed, installed, and operated a 1-km aperture four-element seismo-acoustic array northeast of Seoul, Korea. Joint analysis of the seismic and acoustic recordings can be particularly important in identifying and locating industrial blasting sources. Results from this research array are being used to assess the importance of co-located seismic and acoustic sensors and to determine the utility of small aperture arrays for regional monitoring. In the two months analyzed, there were many more acoustic signals than seismic. Approximately 1/4 of all seismic signals is associated with an acoustic arrival and is presumed to be from mining regions. The vast majority of seismo-acoustic observations come from sources in the 30 - 200 km range in contrast with the shadow zone of no acoustic returns predicted by average atmospheric models. Event location is based upon regional phase identification using the array and back azimuth estimates from both the seismic and acoustic data. Despite the small size of the array, event clusters are identified at regional distances. Waveform comparisons of these clusters indicate that the events are from common source areas. Within the event clusters, there is more event-to-event variation in the acoustic than the seismic signals suggesting the importance of variable atmospheric propagation. The high-Q path of the Korean Peninsula results in regional seismograms that have significant energy to frequencies as high as 16 Hz. The results from this study suggest that small aperture seismo-acoustic arrays such as those similar arrays at Lajitas, Texas (TXAR) and at Mina, Nevada (NVAR) can be important tools in improving

Key Words: Seismo-acoustic, array, regional monitoring, infrasound

OBJECTIVE

The objective of this joint Southern Methodist University (SMU) and Korea Institute of Geology, Mining and Materials (KIGAM) program is to design, procure, integrate, test, install and operate a seismo-acoustic array in the Republic of Korea in order to create a ground truth database as has been done for Lajitas, Texas (TXAR).

RESEARCH ACCOMPLISHMENTS

Array Description The Korean Peninsula provides a unique laboratory for studying regional seismic wave propagation problems in the context of the Comprehensive Nuclear-Test-Ban Treaty (CTBT). There are numerous three-component 40 or 100 samples/s broadband seismic stations in the region operated by KIGAM (Figure 1, closed triangles) as well as the new seismo-acoustic array (CHNAR) jointly operated by SMU and KIGAM. A variety of natural and man-made sources provide ample opportunity for characterizing both wave propagation and source effects within the region (Figure 1, circles and x's).

The focus of this current work is on the analysis of the seismo-acoustic data gathered from the recently installed seismo-acoustic array, CHNAR, in the far north of the Republic of Korea (Figure 1). The array has four-sites about 1 km apart (Figure 2a). Each site has a vertical GS-13 seismometer and a surface acoustic hose array. Data is transmitted from the sites using 2.4 GHz spread-spectrum radios to the central hub. There at the array hub, the data from all the stations are combined, formatted into an Alpha protocol data stream, and then transmitted to the Korea National Data Center by an additional set of spread spectrum radios and a leased telephone line. At the Data Center, CHNAR data is forwarded to SMU.

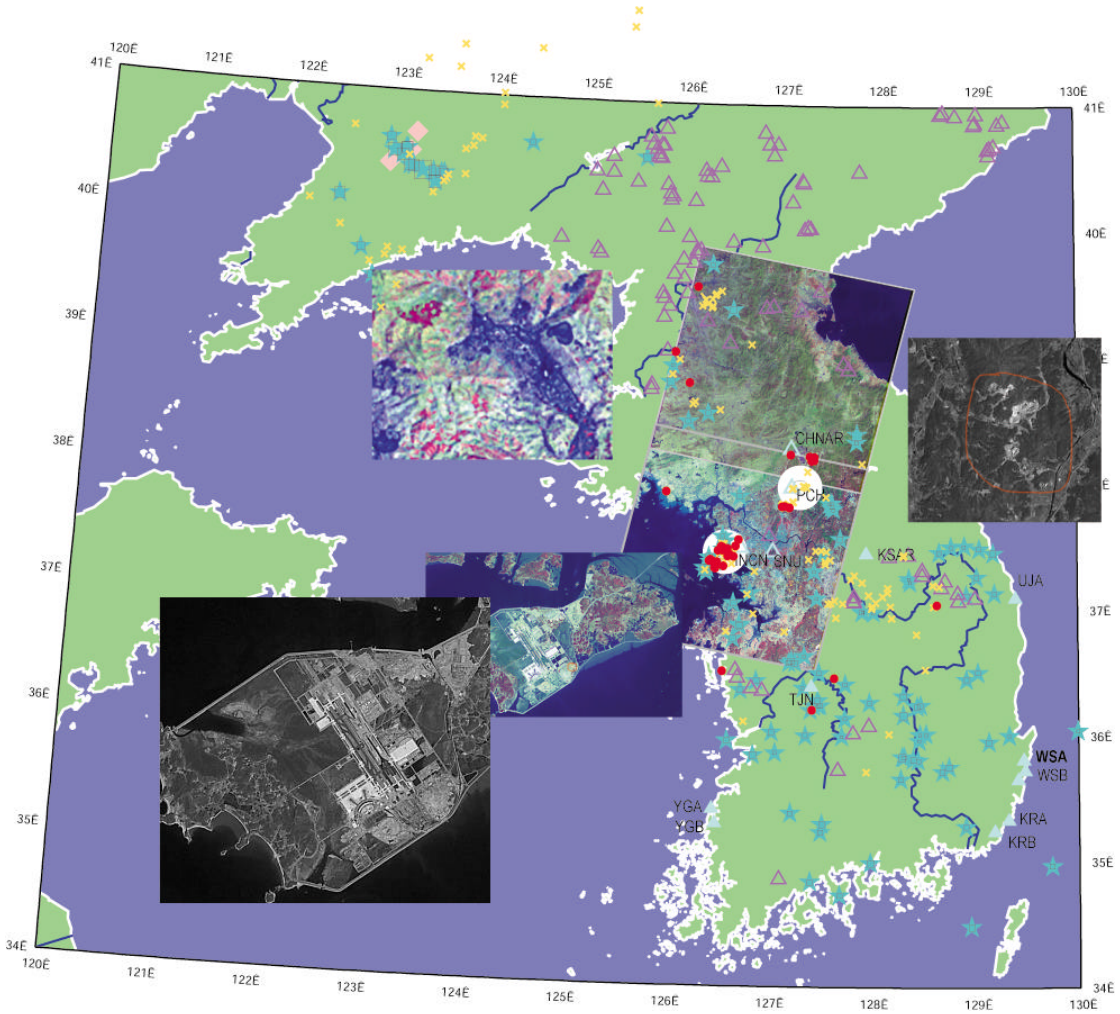

Figure 1. Map of Korean Peninsula that includes the new seismo-acoustic array, CHNAR, the IMS array, KSAR, as well as a number of broadband stations. Superimposed on the map are a number of events including those from this study designated as closed -red circles (seismo-acoustic) and yellow x's (seismic only). Events from KNDC bulletin are marked as blue stars. Ground truth studies based on event locations are highlighted as white circles. Accompanying Landsat images for these regions are also plotted.

The array central element (CHN00) is shown in Figure 2-right. The seismometer is emplaced at the bottom of a 10 m cased borehole. An eleven-element hose array (25' each hose) is deployed at the surface for the purpose of reducing wind noise. At most sites, the hose arrays are covered by low growing grasses. A 1-meter fence to protect the array from intrusion surrounds each hose array (not shown in the figure). The area around the array experiences little cultural activity other than rice farming. The hose array is connected to an acoustic sensor suspended in the borehole. All sites operate on solar charged batteries and telemeter the data to the central hub. Seismic and infrasound channels are sampled at 40 Hz thus providing high-frequency data for regional analysis. A weather station at the hub records local temperature, wind speed and direction.

At sites CHN00, CHN01 and CHN02, the seismometer boreholes are grouted into competent Proterozoic mica schists. Site CHN03 is in a localized weathered Quaternary Basalt flow that appears to affect the regional signals above 10 Hz. .

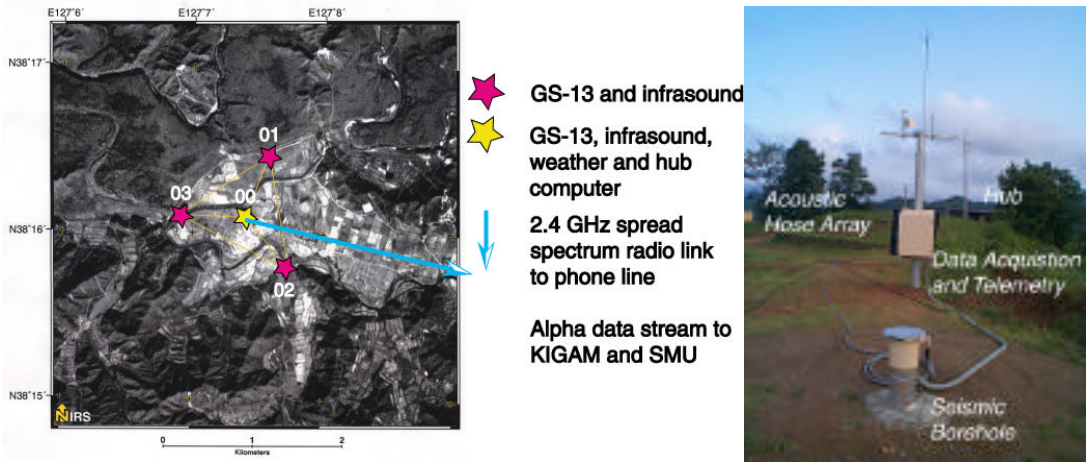

Figure 2 Left: The three outlying sites (CHN01, CHN02, CHN03) are shown in pink. The central site (CHN00) includes the array hub. The blue arrow indicates a radio link to a commercial phone line. Right: The annotated picture of the central site shows a typical site. The borehole contains the GS-13 and the acoustic sensor. The acoustic hose array is on the surface (middle left). The pole-mounted enclosure includes batteries, solar panels, digitizer, and spread spectrum radio. The radio antenna and GPS antenna are mounted on the left of the top crosspiece. The thin finger-like pole at the top is for lightning protection. In the background the mast for the array hub and weather station is positioned just outside the hub building.

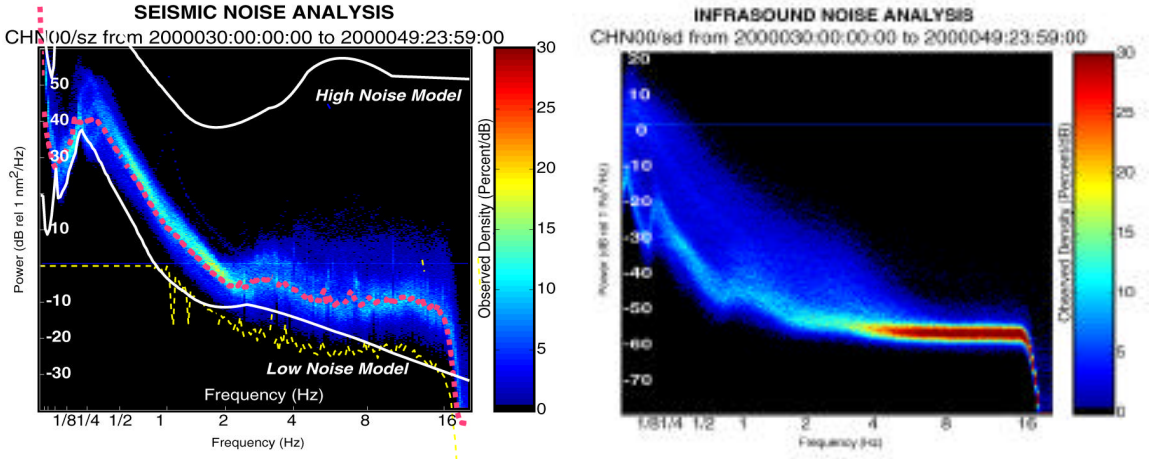

Figure 3: Seismic and acoustic noise estimates from array element CHN00. Colors in the plot represent the observed power-normalized probability density at each frequency from the 20-day analysis. The median for the seismic noise is represented by the red dotted line. The left image is for the seismic data and the right image is for the infrasound data.

Seismic and infrasound noise analysis was done for the twenty-day period from Jan 30, 2000 to Feb 18, 2000, while the site was snow covered. This time period was divided into 10-minute non-overlapping blocks. In each 10 minute block, a 50% overlapped, 104.8s block Welch method was used to estimate the noise spectrum. The resulting noise estimates for one site after instrument correction are shown in Figure 3. Some seismic noise blocks approach the low noise model (as shown by the range of blue values) but the most frequently observed noise level (shown by the red dotted line) is 10 or more dB above this model. Seismic noise levels at CHNAR are well below the high noise model (the upper white line in Figure 3) consistent with competent rock at a remote inland location. The infrasonic noise varies over a much broader range than the seismic noise. Microbarom noise shows as a peak between 1/4 and 1/8 Hz. Above 4 Hz, the infrasound noise spectrum flattens into instrument noise, probably due to the 50-foot aperture of the noise reduction hose array. The effect of the anti-alias filters at 16 Hz is apparent in both plots.

For this time period, the seismic noise spectral variance increases with frequency while the infrasound noise spectral variance decreases with frequency. For seismic noise, the high frequency variance probably reflects local noise sources. For infrasound noise, the reduced high frequency variance is due in part to the effects of the hose arrays. The general characteristics of the noise data for the entire array are well represented with the results from site CHN00. There are additional inter-array variations reflective of the local effects. For example, CHN03 shows increased noise levels above 10 Hz resulting from the emplacement of the seismometer in the shallow (~15 m thick) volcanic layer.

Types of Signals The CHNAR array has contributed significantly to the accurate location and identification of local, regional, and teleseismic signals from a variety of seismic and infrasound sources.

An example of seismo-acoustic signals is given in Figure 4. In this case, the event was first located using the seismic data; distance was determined from the L_g-P time and back azimuth from FK analysis. The acoustic data was then searched for an associated arrival at 414.7s (the expected acoustic arrival time) and a similar back azimuth. This particular event comes from the NE at an approximate distance of 130 km.

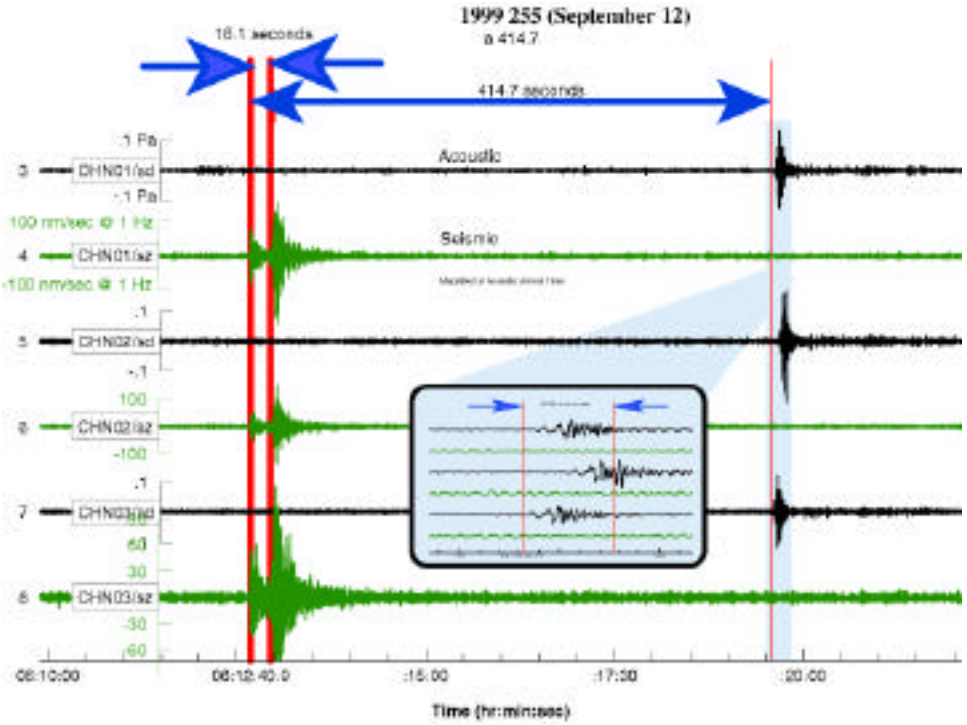

Figure 4: A regional seismo-acoustic signal recorded at CHNAR. The green traces are the seismic channels and the black traces are the infrasound signals. The infrasound arrivals are expanded in the small inset at the center of the figure. Black traces (acoustic) have be shifted relative to absolute time to fit them on the plot. All traces have been filtered in the 0.5 to 5 Hz band.

There are many more infrasound signals than there are seismic or seismo-acoustic. Many of these are distinct and easily recognizable from their waveform although their source or location is unknown. As an example, Figure 5, is a narrow band exponentially decaying signal with a 3.3 Hz frequency. Coupled with its FK direction, it would be easily recognizable should it repeat. In this example, there are no associated seismic signals.

Seismic, Seismo-Acoustic and Acoustic Event Statistics The two month period from January 1 to February 29, 2000 was chosen for a reconnaissance analysis of all seismic and seismo-acoustic signals. This time period overlaps with the period used for the noise analysis (Figure 3). This signal analysis was done to quantify the CHNAR's utility to detect and associate seismic and infrasound signals. One of the primary goals was to assess the identification of man-made signals from mining operations. Since regional

signals were the primary interest, both the seismic and infrasonic data were filtered from 1 to 5 Hz matching the expected best SNR and the flat part of the noise spectra (Figure 3). An analyst reviewed the data to form events.

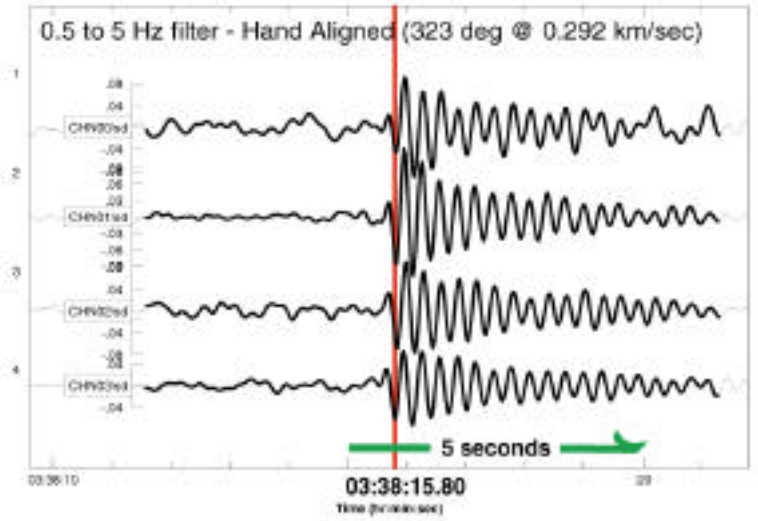

Figure 5: An example of a narrow band infrasound signal recorded at CHNAR. The signals have been time aligned in an attempt to estimate phase velocity and back azimuth.

The analyst formed events based on an interpretable seismic arrival. Regional phases such as P_g, P_n, PmP, L_g and R_g were identified based on arrival order, frequency content and FK phase velocity estimates. For each of the associated phases, FK back azimuth estimates had to be consistent. A crude distance estimate was made using L_g-P time and multiplying by 8 km/s. This procedure provided an initial event location that then triggered a search for associated infrasound arrivals in a window defined by with group velocities of 250 to 400 m/s. If a coherent infrasonic signal was found in this window with a FK back azimuth consistent with the seismic estimates, then a seismo-acoustic event was formed.

The number of seismic events averages about 4 per day with as many as 12 in any one day (Figure 6). There are few events from day 35 to 41 (Feb 4-10) during the Spring Festival, a Korean national holiday. This seismic lull and the dramatic activity increase for the week prior to the holiday suggests that many of these seismic events may be man-made.

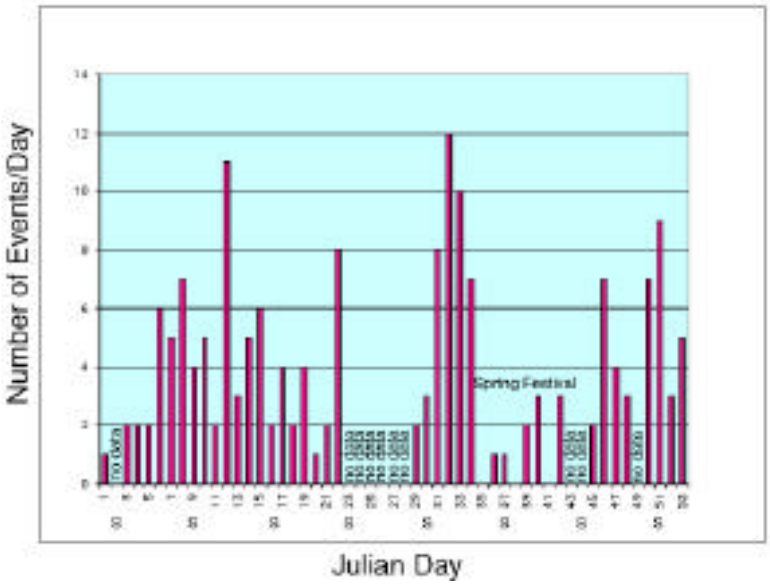

Figure 6: Number of seismic events as a function of Julian Day for the time period of the study, January-February 2000.

The man-made source is further supported by the origin time of day. An hourly binned histogram (Figure 7a) shows that the maximum number of seismic events, 25, occurs during the noon hour local time. The number of events increases dramatically in the mid-morning hours and then stops abruptly after 6 pm local time. A similar plot was made for the seismo-acoustic events and is reproduced in Figure 7b. All but one of the seismo-acoustic events identified during this study occurred during daylight working hours, 7am until 6 pm local time. These observations indicate that most of the signals received from CHNAR are associated with industrial operations such as mining.

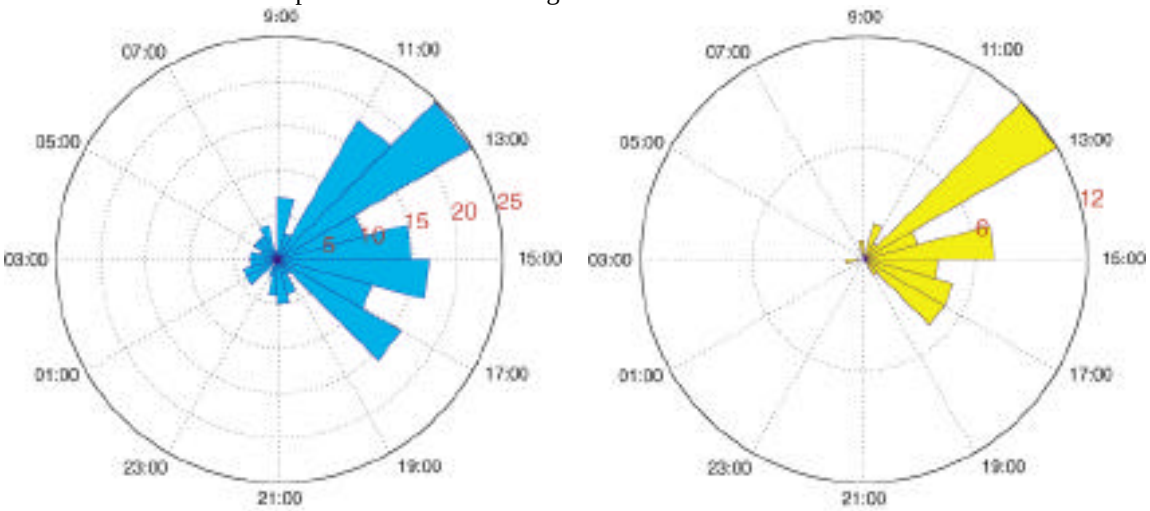

Figure 7: a) The number of seismic events identified using CHNAR during January and February are plotted as a function of local time in the image to the left (blue). b) The total number of seismo-acoustic events identified during this study as a function of local time is plotted to the right (yellow). Both plots indicated a concentration of events during local working hours.

The spatial distribution of seismic (red x) and seismo-acoustic (yellow o) events identified in the study are plotted as a function of average azimuth from CHNAR and L_g-P time (range ~ [L_g-P time] x 8 km/s) in Figure 8. Although all interpretation is based only on CHNAR, a single small-aperture array, the events cluster into a number of well-defined groups. Groups 1,4,5,6, and 11 include seismo-acoustic events constrained to day time hours and therefore suggest either a mining or construction source. Group 2 events occur at all hours but include no seismo-acoustic signals. Therefore they are probably associated with natural seismicity.

An average of 4 events/day (157 total events) occurred during the period-analyzed (Figure 8). Only 22% (35 events) are seismo-acoustic and have associated infrasound signals. Only one of the seismo-acoustic signal occurs at night and it is a local high frequency event.

It was obvious on even a casual perusal that on any day, there are many more infrasound signals than seismic. One week (19-25 February 2000) of infrasound data was comprehensively reviewed with the analyst examining all of the recorded infrasound data. An infrasound event was defined as visually correlated coherent signals across the array. For each infrasound event the analyst made an FK measurement of back azimuth and phase velocity summarized in Figure 9. 263 infrasound events were observed for this seven day period where the number of events a day ranged from 13 to 84, four to ten times higher than the number of seismic events. Like the seismo-acoustic events, the acoustic only events mostly occur during normal workday hours. The observed azimuths are from a very narrow range, primarily from the northwest, which is the direction of the prevailing winds during this time period.

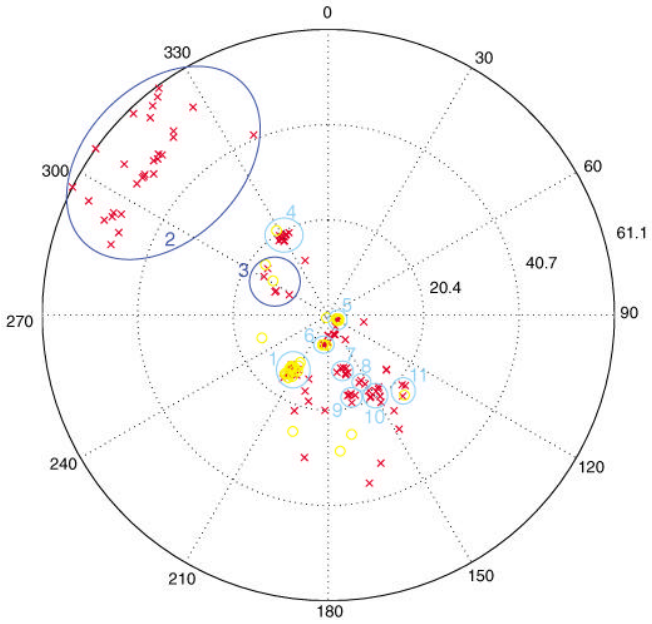

Figure 8: Event groups and locations for January-February 2000 using CHNAR. Average azimuth was determined from all associated arrivals. The distance (radius) is plotted as L_g-P time in seconds. A rough distance conversion may be calculated made by multiplying the plotted L_g-P time by 8km/s. The red x's are seismic events while the yellow o's are seismo-acoustic events. The events are subjectively divided into 11 groups. Dark blue ellipses indicate that some events within the group occurred during the night. Light blue ellipses indicate all events in the group occur during the day.

Event Clusters Event location and time-of-day clusters provide an opportunity to characterize seismic waveforms and infer the characteristics of sources. Clusters such as #1 in Figure 8 with the high number of seismo-acoustic events might be construction or mine related. Clusters such as #2 with no associated infrasound signals, and day and night occurrence might be earthquakes. In order to investigate these clusters further, waveforms for each cluster may be examined.

Events in Group 2, over 400 km to the NW of CHNAR, occur at all hours and have no associated infrasound signals. Waveforms for these events (Figure 10a) are very similar although the peak amplitudes span a factor of five. The modest P_g arrival and the following large L_g wave packet arrival are easily identified. At this distance an emergent P_n is the first arrival and can barely be seen in the second seismogram. For smaller events it is not discernable above background noise. For smaller events the range estimate is too near, when P_g is mistaken for the P_n first arrival. Inspection of the locations in Figure 8 suggests two linear trends in the locations for Group 2. The closer events are those for which P_g was mistakenly interpreted as a first arrival. When these mislocated events are moved to the correct range, the events form a single linear trend that overlaps the Tan Lu Fault in SE China. This further supports earthquake (non-industrial) source hypothesis.

The regional seismograms were bandpass filtered to investigate the frequency content of the regional arrivals. Figure 10b illustrates one of the events filtered into bands 0.05-0.5 Hz, 0.5-1 Hz, 1-2 Hz, 2-4 Hz, 4-8 Hz, 8-16 Hz. Similar results were found for the other events in the group. This display illustrates the relative spectral energy of Pg and Lg. The shear energy dominates the P energy at in all filter bands. This is consistent with an explosion source.

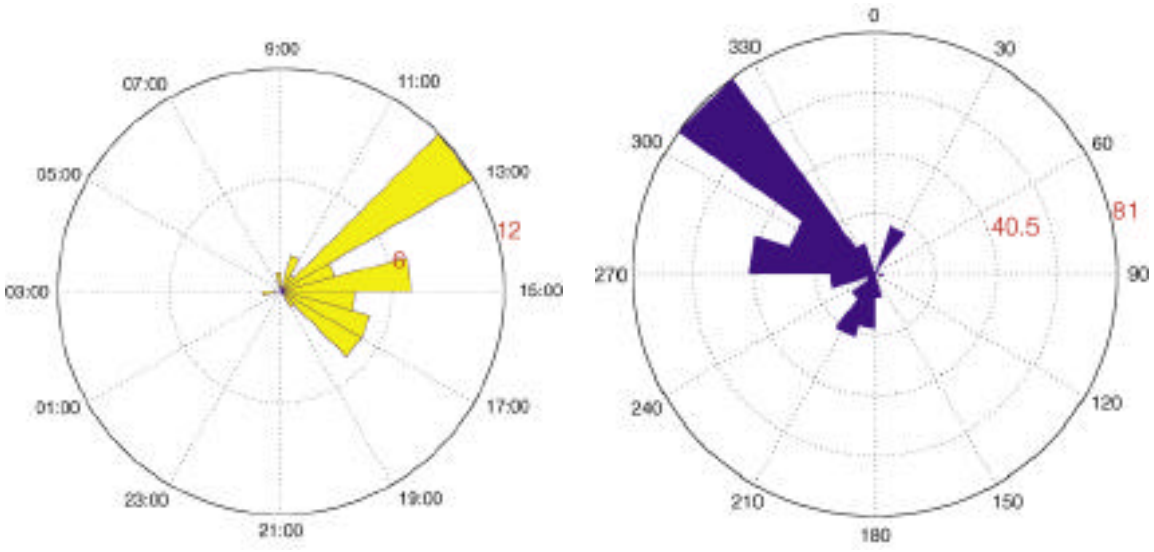

Figure 9: Summary results from the analysis of the infrasound data. (a)The left figure plots the number of events in hour bins (local time). (b)The right figure plots the number of events coming from different azimuths with respect to CHNAR.

An example from Group 1 (Figure 11a) compares vertical seismograms for signals hypothesized to be industrial or construction explosions. Most of the events in this group have associated infrasound signals (the seismo-acoustic source case). The source is approximately 120 km away and the waveforms include P_g, PmP and L_g arrivals. Although seismograms are similar, subtle differences in arrival time and waveshapes within the group warrant further study. The event-to-event amplitude range is small, no more than 6 dB.

The example Group 1 bandpass filtered seismogram (Figure 11b) show strong high frequency P waves and indications of an intermediate frequency surface wave. Both observations are consistent with an explosion source. Based on these observations the estimated source location was investigated for possible sources (ground truth investigation). In this region, construction is in progress for a new international airport to serve Seoul. At either end of the airport are two small mountains that are being explosively removed. Close-in measurements of one of these explosions validated them as the source of events for Group 1. This location is shown in Figure 1 along with the overhead imagery of the new airport.

Infrasound waveforms for all sites and three of the Group 1 events in Figure 11 are displayed in Figure 12. The move-out across the array and strong visual coherence is apparent and is used to identify an infrasound event within the predicted time window. Signal amplitude covers a narrow range of 0.1 to 0.2 Pascals. Although there is significant event-to-event waveform variation, single events show good correlation across the array event at relatively high frequencies. The signals are relatively high frequency (Figure 12b) with energy centered from 1 to 8 Hz. Similar spectra were found for the other infrasound signals from this and other clusters.

A similar investigation of the signals in Group 6, which included many seismo-acoustic signals, suggested a mining or construction sources. Investigation in this region followed by local measurements validated the source of signals from Group 6 as a granite quarry. The overhead imagery for this location is also included in Figure 1.

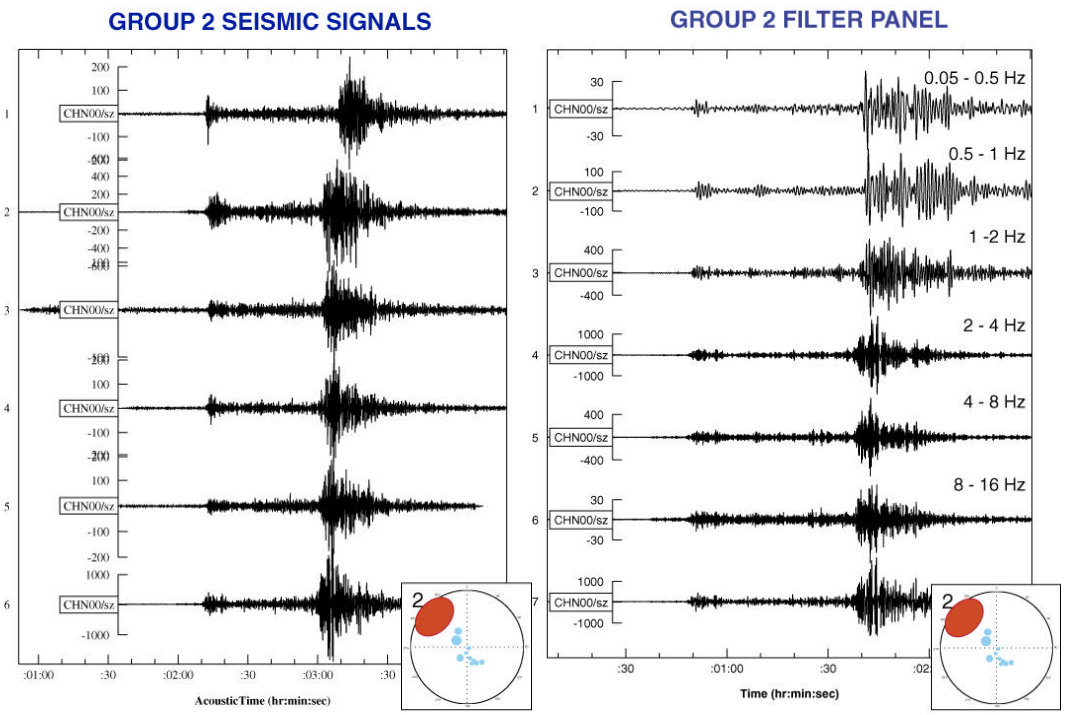

Figure 10: (a) Comparison of vertical seismograms recorded at Site CHN00 for six events from Group 2 in Figure 8. (b) Bandpass filtered seismograms of one event from Group 2.

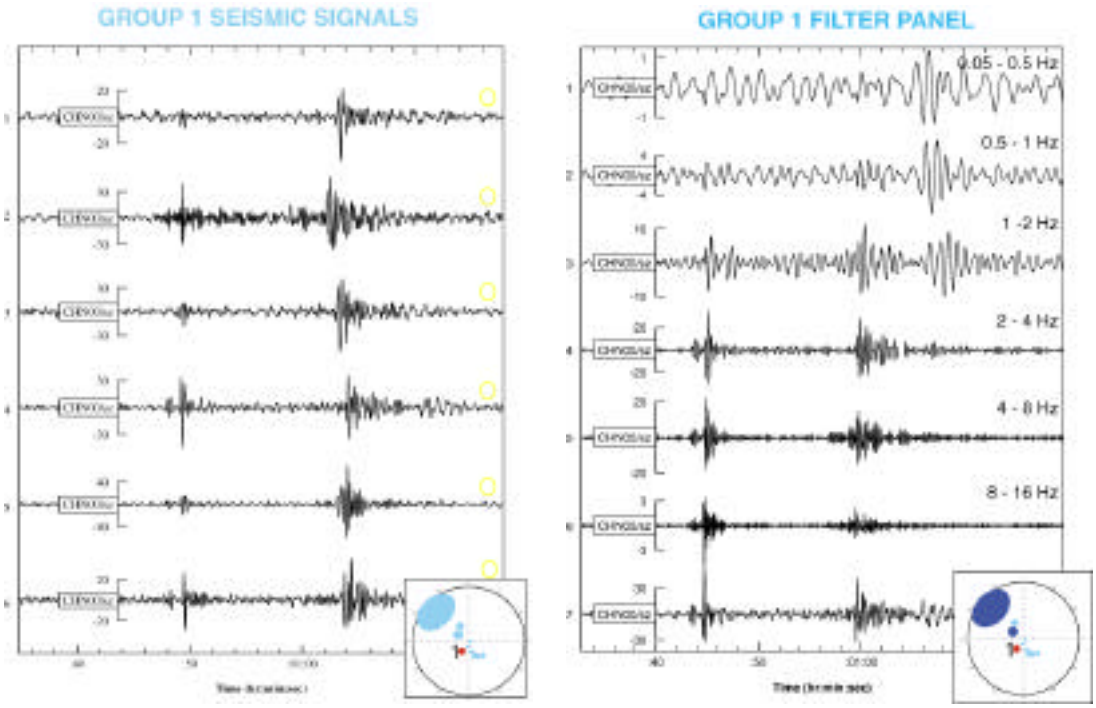

Figure 11: (a) Comparison of vertical seismograms recorded at Site 00 for six events from Group 1 in Figure 8. (b) Bandpass filtered seismograms of one event from Group 1.

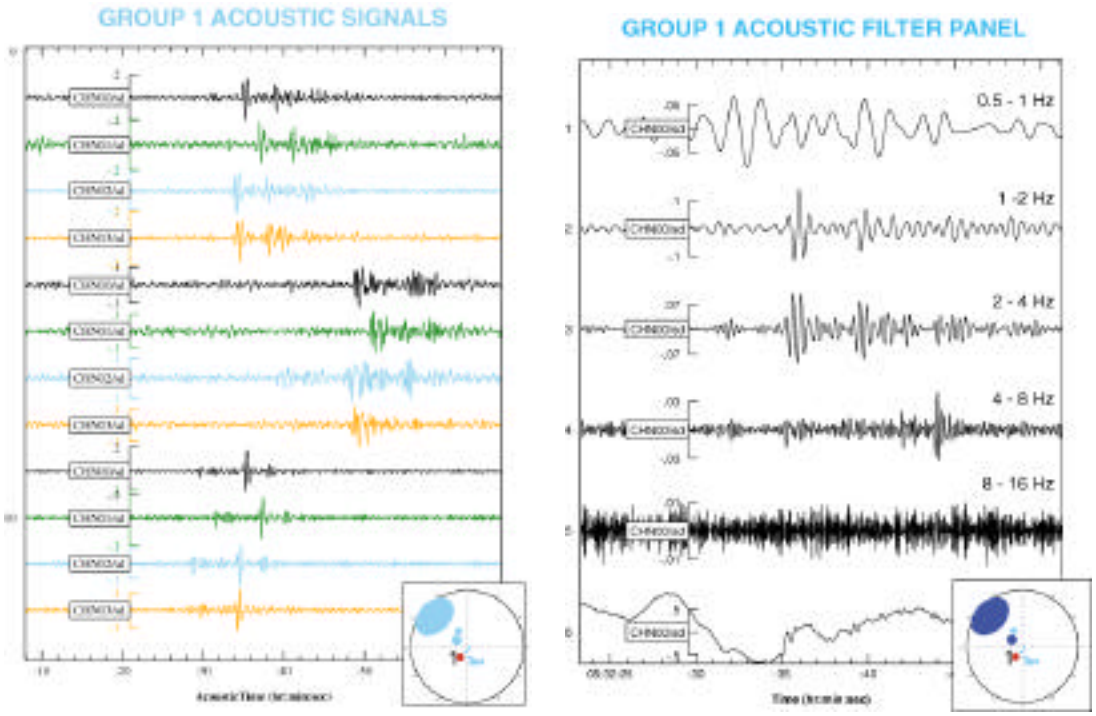

Figure 12: (a) Comparison of infrasound signals recorded across CHNAR from three Group 1 events (b) Bandpass filtered infrasound signal from one of these events.

CONCLUSIONS AND RECOMMENDATIONS

A small aperture array for seismo-acoustic signals has been designed, constructed and installed. Many seismic and infrasonic signals are observed daily. Nearly a quarter of all seismic signals has associated infrasonic arrivals. Most occur during normal local working hours. There are many more infrasonic signals than there are seismic. These observations suggest that a great deal of the activity observed is manmade.

Event locations based upon data from CHNAR cluster. Investigation of these clusters indicates great similarity in seismic waveforms. Two clusters of seismo-acoustic events were used to trigger a successful search for ground truth information. One source region was associated with construction blasting at a new airport and the second was a granite quarry.

Many of the seismo-acoustic signals are observed in the distance range of 50 to 200 km. Average atmospheric velocity models do not predict ray paths that return in this distance range. This observation and the correlation of the wind direction and predominant direction of low altitude winds suggest that local ducting may be important for these signals.

Additional work is needed in the interpretation and modeling of seismic and infrasound signals. Emphasis will be placed on gathering additional ground truth information to aid in this study.

ACKNOWLEDGEMENTS

The work of Karl Thomason, Nin-Chul Shin, Jason McKenna, Il-Young Che, Paul Golden, Dong Kyun Kim, Yong-Sung Kim, and Jung-Ho Park in the design, installation and operation of the array are acknowledged. This work could not have been completed without this enthusiastic and cooperative team not to mention significant helpings of kimchi.